

Numerical and Experimental Study of Microwave Drying of White Oak (*Quercus Alba*)

D. Jia *Faculty of Forestry & Environmental Management, University of New Brunswick, PO Box 44555, Fredericton, New Brunswick, Canada, E3B 6C2*

M. T. Afzal *Faculty of Forestry & Environmental Management, University of New Brunswick, PO Box 44555, Fredericton, New Brunswick, Canada, E3B 6C2, Email: mafzal@unb.ca*

ABSTRACT

The microwave drying of white oak (*Quercus Alba*) was studied using both numerical model and experimental data. A 2-D comprehensive heat and mass transfer model was developed to simulate the free liquid, vapor, and bound water movement in microwave drying of white oak specimens. The experimental and model results showed that, for white oak, moisture movement was easily impeded and high internal vapor pressure occurred. The internal vapor pressure was affected by sample dimension (length and thickness). At the same input power density, the internal pressure achieved in the core increased with the increase in sample length or thickness. However, as compared with sample length, sample thickness has less effect on pressure change because of the high ratio of permeability between longitudinal and transverse directions.

INTRODUCTION

A number of methods are in commercial use for drying hardwood lumber, such as conventional kiln drying, vacuum drying, RF drying and microwave drying. Microwave drying offers an opportunity to increase the rate of drying because the energy is absorbed throughout the volume, and the heat is generated directly within the material being dried. Microwave drying of wood has been studied since 1960s, and is an effective and fast way of wood heating process (Barnes, et. Al., 1976; McAlister and Resch 1971).

In order to improve process performance and reduce energy utilization, it is desired to develop mathematical models to evaluate relative performance of microwave drying of wood. The interaction between microwave radiation and wood has been numerically studied by solving Maxwell equations (Perre 1996; Zhao and Turner 2000). The process of wood drying involves simultaneous transport of heat and mass through the wood (Gong and Plumb 1990). The developed comprehensive heat and mass transfer models in conventional drying have been used in some studies to predict the microwave drying process. Turner and Ferguson, 1995 combined the existing

comprehensive 2-D heat and moisture transfer model with Maxwell's electromagnetic equations in the modeling of microwave drying of wood. To simplify the comprehensive models, Koumoutsakos et al., 2001 assumed negligible capillary water transportation in radio frequency /vacuum drying of thick lumber. They concluded that moisture was mainly removed by vapor transport, and thus capillary transportation could be negligible. However, there has been no further discussion about simplification of the comprehensive models in recent model studies.

In the literature, strong vaporization was highlighted in the microwave drying of green wood. Antti, 1992; 1995 experimentally studied the internal vapor relative pressure, and reported 70kPa with local temperature 125°C and moisture content 38% for pine heartwood. Perre and Turner, 1989 gave the experimental internal vapor relative pressure for combined microwave and convective drying of spruce heartwood as approximately 200kPa with the local temperature approximately 130°C and moisture content 38%. However, the relationship between internal vapor pressure with other factors, including species, power level, moisture content, and dimension, was unclear in the literature. Antti, 1992 proposed that the internal

gaseous pressure was due to the power level, and demonstrated that the pressure was independent of specimen dimension for ash and oak, but increased with increasing piece length for beech.

This paper comprised numerical and experimental study of microwave drying of white oak (*Quercus Alba*). White oak is a less permeable wood species with tyloses (cell membrane) clogging the cell lumen, and hard to dry. It is also an expensive species, highly prized for bridges, furniture, and flooring. A 2-D heat and mass transfer model was developed to investigate the liquid flow due to capillarity, vapor convective bulk flow in the drying process, and also to study the effects of sample dimension, power level on wood temperature and internal vapor pressure.

MATHEMATICAL FORMULATION

The main assumptions included in this model are given in Jia, 2006. Based on the composition of wood cell and moisture, wood specimen can be modeled as a solid matrix where the void volume, formed by cell lumen, is initially filled partly by internal gas and partly by liquid water.

Conservation Equations

The mass and heat transfer during microwave drying include free water and vapor convective flow, bound water and vapor diffusion movement, and heat movement caused by conduction and mass transfer. Whitaker, 1977 discussed in detail the macroscopic conservation equations that govern heat and mass transfer phenomena in porous media. The conservation equations for a multiphase flow were obtained by volume averaging technique as,

$$\frac{\partial \phi_g \rho_v}{\partial t} + \nabla \cdot (\rho_v \bar{u}_v) - \nabla \cdot \left(\rho_g D_{eff} \nabla \left(\frac{\rho_v}{\rho_g} \right) \right) = \dot{m}_i + \dot{m}_b \quad \dots(1)$$

$$\frac{\partial \phi_g \rho_a}{\partial t} + \nabla \cdot (\rho_a \bar{u}_a) - \nabla \cdot \left(\rho_g D_{eff} \nabla \left(\frac{\rho_a}{\rho_g} \right) \right) = 0 \quad \dots(2)$$

Energy conservation equation is obtained by forming an energy balance for a fixed control volume,

$$\frac{\partial (\rho_{wood} \epsilon_{pwood} T)}{\partial t} + \nabla \cdot ((\rho_v h_v + \rho_a h_a) \bar{u}_g + \rho_l h_l \bar{u}_l + \rho_b h_b \bar{u}_b) = \nabla \cdot (\lambda_{eff} \nabla T) + Q \quad \dots(3)$$

Internal Heat and Mass Transfer

Extended Darcy's law, by using relative permeability, provides expression for the free liquid and gas phase velocities as following,

$$\bar{u}_g = - \frac{K_g k_{rg}}{\mu_g} \nabla p_g \quad \dots(4)$$

$$\bar{u}_l = - \frac{K_l k_{rl}}{\mu_l} \nabla p_l = - \frac{K_l k_{rl}}{\mu_l} \nabla (p_g - p_c) \quad \dots(5)$$

The bound water migrates through the cell-wall matrix via a diffusion mechanism, which is present for

moisture contents below the FSP. Fick's first law models the diffusive transport:

$$J_b = \rho_b \bar{u}_b = - \rho_s D_b \nabla M \quad \dots(6)$$

From the assumptions, the binary mixture of vapor and air is considered as an ideal mixture of perfect gases. So the state equations of gas exists

$$p_g = \rho_g R_g T \quad \dots(7a)$$

$$p_{air} = \rho_{air} R_{air} T \quad \dots(7b)$$

$$p_v = \rho_v R_v T \quad \dots(7c)$$

The total internal gaseous pressure (p_g) consists of partial vapor pressure and partial air pressure. The saturated water vapor pressure within the solid is shown as (Siau 1995):

$$p_v^{sat} = - \exp(53.421 - 6516.3/T - 4.125 \ln T) \dots(8a)$$

In the absence of free water, significant vapor pressure depressions are predicted, mainly at the lower temperatures (Blasi 1998),

$$\frac{p_v}{p_v^{sat}} = \exp(7.884 - 0.142T + 23.63 \times 10^{-5} T^2) \cdot (1.0327 - 67.4 \times 10^{-5} T)^{0.2M} \quad \dots(8b)$$

The pressures of each phase are related to each other via the capillary pressure (P_c) in wood cell. The capillary pressure is a function of wood moisture content (Spolek and Plumb 1981):

$$p_c = 1.2 \times 10^4 (S + 1.2 \times 10^{-4})^{-0.61}, \quad S = \frac{M - M_{fsp}}{M_{max} - M_{fsp}} \quad \dots(9)$$

Enthalpy functions for each of the components in Eq. 5 were defined in terms of temperature. For wood drying, the zero enthalpy reference state of each component was chosen to be 273.15K and 101,325 Pa; the enthalpies of air, free liquid water, and dry wood are then,

$$h_{air} = Cp_{air} (T - 273.15) = 1010.0(T - 273.15) \dots(10a)$$

$$h_{liquid} = Cp_{liquid} (T - 273.15) = 4180.0(T - 273.15) \dots(10b)$$

$$h_s = Cp_s T = 1360.0(T - 273.15) \dots(10c)$$

Stanish et al., 1986 gave correlations for both the heat of vaporisation Δh_{vap} (J/kg) and the dew point temperature T_{dew} (K),

$$\Delta h_{vap} = 2.792 \times 10^6 - 160 T - 3.43 T^2 \quad \dots(11)$$

Dew point temperature was correlated with partial water vapor pressure by

$$T_{dew} = 230.9 + 2.1 \times 10^{-4} p_v - 0.639 p_v^{1/2} + 6.95 p_v^{1/3} \dots(12)$$

Systems of Equations to be Solved

The detailed procedure is described by Jia, 2006. The derived coupled moisture, air, and energy balance partial differential equations have the following form:

$$\frac{\partial \rho M}{\partial t} - \nabla \cdot \left(\left(\rho \frac{K_i k_{rl}}{\mu} + \rho_s \frac{K_s k_{rg}}{\mu_s} \right) \nabla p_g \right) - \nabla \cdot \left(\left(\rho D_b - \rho \frac{K_i k_{rl}}{\mu} \frac{\partial p_c}{\partial M} \right) \nabla M \right) = \nabla \cdot \left(\rho_g D_{eff} \nabla \left(\frac{\rho}{\rho_g} \right) \right) \quad \dots\dots\dots(13)$$

$$\frac{\partial \rho_g p_g}{\partial t} - \left(\rho_g \rho R_u + \frac{\partial \rho_g p_v}{\partial t} \right) \frac{\partial T}{\partial t} - \frac{\partial \rho_g p_v}{\partial M} \frac{\partial M}{\partial t} = R_u T \left(\nabla \cdot \left(\rho_{air} \frac{K_s k_{rg}}{\mu_s} \nabla p_g \right) - \nabla \cdot \left(\rho_g D_{eff} \nabla \left(\frac{\rho}{\rho_g} \right) \right) \right) \quad \dots\dots\dots(14)$$

$$\frac{\partial (\rho_{wood} \mathcal{E}_{pwood} T)}{\partial t} - \nabla \cdot \left(\left(\rho_v C_p T \frac{K_s k_{rg}}{\mu_s} + \rho_l C_H T \frac{K_i k_{rl}}{\mu} + \rho_{air} C_{p_{air}} T \frac{K_s k_{rg}}{\mu_s} \right) \nabla p_g + \left(\rho_s D_b C_p T - \rho_l C_H \frac{K_i k_{rl}}{\mu} T \frac{\partial p_c}{\partial M} \right) \nabla M \right) - \Delta T \nabla \cdot \left(\rho_v \frac{K_s k_{rg}}{\mu_s} \nabla p_g \right) = \nabla \cdot (\lambda_{eff} \nabla T) + Q \quad \dots\dots\dots(15)$$

Three independent variables, moisture content M , temperature T , and total internal gas pressure p_g , were utilized in this paper. The moisture content was given as,

$$M = \frac{\phi_l \rho_l + \rho_b + \phi_v \rho_v}{\rho_s} \quad \dots\dots\dots(16)$$

The strong anisotropy ratio of wood in longitudinal to radial permeability makes a two dimensional model necessary. In this study, the transverse (y-direction) and longitudinal (x-direction) directions of the wood were considered. Eqs. 13, 14 and 15 constitute the two-dimensional system of three nonlinear coupled partial differential equations that govern the drying process.

Boundary Conditions

The control domain for the calculations covers only one quarter of the total volume of the sample as a result of the symmetry of the wood sample. As the configuration shown in Fig.1 there are two types of boundary conditions, namely, conditions at the external boundaries, and conditions at symmetry planes. Across the boundary, the fluxes of mass are continuous. In the case of air in the surroundings, the boundary conditions proposed for the external drying surfaces of the sample were assumed to be the following form (Mardini, et.al., 1996):

$$J_v \cdot \bar{n} = k_m (\rho_v^s - \rho_v^\infty) \quad \dots\dots\dots(17)$$

The boundary condition for the energy equation was derived in quite an analogous way as for the mass continuity equation. The total energy flux within the solid at each surface must equal the total energy through the external boundary layer

$$J_e \cdot \bar{n} = h (T^s - T^\infty) \quad \dots\dots\dots(18)$$

The total pressure at the external drying surface was fixed as the chamber pressure,

$$p_g |_s = p_\infty \quad \dots\dots\dots(19)$$

On the symmetry plane all the fluxes were zero:

$$\frac{\partial p_g}{\partial n} = 0, \quad \frac{\partial M}{\partial n} = 0, \quad \frac{\partial T}{\partial n} = 0 \quad \dots\dots\dots(20)$$

Numerical Procedures

In the study of wood drying process, high aspect ratios of the geometry of the wood, high anisotropy ratios, steep moisture and pressure gradient put numerical approach necessary for drying process analysis. To solve the tightly coupled, nonlinear model equations, a CFD code was developed using the finite difference method in MATLAB. With finite difference, Eqs. 15, 16 and 17 were solved as individual uncoupled two-dimensional equations. The coupling terms were all transferred to the right-hand side of the discretized equations, i.e. the other variables in the non-linear term of each conservation equation took the last available values. Since the convective mass flow terms were comparable to or larger than the dispersion terms, the hybrid up-winding scheme was used to keep the discretization stable

$$\nabla T \cdot \nabla p_g = \left(\frac{T_{i,j}^{n+1} - T_{i-1,j}^{n+1}}{\Delta x} \cdot \frac{p_{g,i,j}^n - p_{g,i-1,j}^n}{\Delta x} + \frac{T_{i,j}^{n+1} - T_{i,j-1}^{n+1}}{\Delta y} \cdot \frac{p_{g,i,j}^n - p_{g,i,j-1}^n}{\Delta y} \right) \quad \dots\dots\dots(21)$$

To maintain stability and accuracy, the Crank-Nicholson scheme was used for the dispersion terms:

$$\begin{aligned} \nabla^2 p_g &= 0.5 \left(\frac{p_{g,i+1,j}^n - 2p_{g,i,j}^n + p_{g,i-1,j}^n}{\Delta x^2} + \frac{p_{g,i,j+1}^n - 2p_{g,i,j}^n + p_{g,i,j-1}^n}{\Delta y^2} \right) + \\ &0.5 \left(\frac{p_{g,i+1,j}^{n+1} - 2p_{g,i,j}^{n+1} + p_{g,i-1,j}^{n+1}}{\Delta x^2} + \frac{p_{g,i,j+1}^{n+1} - 2p_{g,i,j}^{n+1} + p_{g,i,j-1}^{n+1}}{\Delta y^2} \right) \\ &= 0.5 (\delta_x^2 p_g^n + \delta_y^2 p_g^{n+1}) + 0.5 (\delta_x^2 p_g^{n+1} + \delta_y^2 p_g^n) \quad \dots\dots(22a) \end{aligned}$$

$$\nabla^2 M = 0.5 (\delta_x^2 M^n + \delta_y^2 M^{n+1}) + 0.5 (\delta_x^2 M^{n+1} + \delta_y^2 M^n) \quad \dots\dots(22b)$$

$$\nabla^2 T = 0.5 (\delta_x^2 T^n + \delta_y^2 T^{n+1}) + 0.5 (\delta_x^2 T^{n+1} + \delta_y^2 T^n) \quad \dots\dots(22c)$$

Input data for model simulation include initial drying conditions, wood properties (such as wood basic density and green moisture content), lumber dimensions and drying conditions (air temperature, humidity and air velocity). The code can simulate the whole drying process, and provide the progress of temperature, moisture content, pressure and moisture gradients. In the process of simulation, for stable calculation there were some limitations on the size of the time step which depend on the velocity of vapor movement.

RESULTS AND DISCUSSION

Model Verification and Drying Process Investigation

In order to testify the validity of the mathematical model, White oak samples were dried in a Panasonic microwave oven, Model NN-S963/S763 with maximum power 1250W. The dimension of experimental specimens was 100 mm long, 25 mm thick, and 50 mm wide. The sample tangential side surfaces were sealed with silicone coating in order that drying would take places only the longitudinal and radial directions.

A FISO Optical Slip-Ring (OSR) system was used to measure the simultaneous temperature of wood specimens. Mass change of specimen during the drying process was measured using an electronic balance connected with a computer. Vapor pressure was obtained using a pressure transducer, OMEGA's PX4202 Series Transmitters ranging 0-100psi, which was connected by a thin tube with the samples. The transducer has a manufacturer reported accuracy of $\pm 0.25\%$ with the temperature tolerance up to 120°C . The environmental conditions in the microwave oven were approximately 24°C and 44% relative humidity before the microwave power was applied. After heating, some specimens were sliced to determine the moisture profiles in the longitudinal or transverse direction. Two power levels, 250W and 375W were chosen to heat the samples quickly to the boiling point. And corresponding initial heat generation (Q) for model calculation were obtained experimentally.

The model simulations results and corresponding experimental data are shown in Fig. 2 to Fig. 6 to verify both the model predictions and appropriate transport parameter values. In the figures, the strong coupling of all variables are highlighted: the absorbed power changes the temperatures in Fig. 3, leading to an increase in both the vapor pressure and pressure gradients (Fig. 4). These gradients induce, respectively, convective vapor and liquid fluxes that are responsible for moisture release (Fig. 2). The comparison between numerical and experimental results showed good model predictions of drying curve, temperature, and internal vapor pressure.

Fig. 4 compares the predicted internal gaseous relative pressure with experimental result in microwave drying of white oak. The figure demonstrates that microwave drying causes high internal gaseous relative pressure in white oak sample, almost 132kPa at power 250W. Fig. 4 show lower internal gaseous relative pressure values by model prediction than the experimental results in the first period of drying process. This is probably due to the experimental setup for pressure measurement. The pressure transducer is connected to the sample by thin tubes through a connector. All the connections, including the connections between sample and tube, tube and tube, and tube and transducer, affect the pressure reading

especially at the beginning period when the vapor pressure increases. Another reason for this pressure difference may be the assumption that wood is homogeneous. Wood is a complex material, and is composed of cells connected by small diameter pits. This phenomenon may cause high pressure at the beginning of drying until water goes through the pits and moisture escapes freely.

Although there is difference between experimental results and model predictions of internal gaseous pressure, especially in the beginning period, the model predictions for other periods are consistent with the experimental data. Generally, the model gives reasonable predictions of internal gaseous pressure in the drying process.

For moisture distribution, the agreement between model prediction and experimental data is evidently good (Fig. 5 and Fig. 6). From the analysis and comparison between model prediction and experimental data, it is concluded that the numerical model for moisture and heat transfer can be suitably used to predict the variables of moisture content (M), temperature (T) and gaseous pressure (P_g) at different drying conditions. The boundary conditions described above can correctly describe the moisture and heat transfer process through the material surfaces.

Effect of Sample Dimension

To investigate the effect of sample dimension on internal gaseous pressure, microwave drying of wood samples (in different dimension) was studied using the developed 2-D model in the preconditions of same microwave power density in the wood and similar boundary conditions (such as air flow and chamber temperatures). The model prediction results are shown in Fig. 7 and Fig. 8.

In Fig. 7 and Fig. 8, at the condition of same microwave power density ($280\text{kW}/\text{m}^3$), when the simulated white oak sample length changes from 0.1 m to 0.2 m to 0.4 m, the maximum internal gaseous relative pressure (obtained by model calculation) increases from 136.0kPa to 273.7kPa to 386.4kPa; and the internal temperature increases from 125.7°C to 141.4°C to 150.5°C respectively. With the sample length doubles, the internal gaseous pressure increases more than one atmosphere pressure. Fig. 8 show the effects of white oak sample thickness on internal gaseous pressure. The internal gaseous pressure in wood increases with increasing sample thickness. Probably, the thicker sample decreases the temperature loss in the sample core, and affects the internal gaseous pressure. The effect of sample thickness on the internal gaseous pressure is not significant compared to the effect of sample length. Fig. 8 gives that the internal gaseous pressure increases only from 136.0kPa to 161.3kPa when the simulated sample thickness changes from 25 mm to 50 mm.

CONCLUSION

A 2D comprehensive model was developed to investigate the free water, vapor, and bound water movement in microwave drying of white oak. The numerical and experimental results show that the internal gaseous pressure and temperature in the wood are mainly governed by wood permeability, power level, and sample dimension. Sample dimension affects the internal pressure. At the same microwave power density, greater sample length decreases the integrated permeability of the sample, and greatly increases the internal pressure achieved in the core. Increasing sample thickness also increases the sample's internal pressure at the same power density; compared to sample length, sample thickness has less effect on pressure change because of the high ratio of permeability between longitudinal and transverse directions.

ACKNOWLEDGEMENT

The authors acknowledge the financial support from Natural Science and Engineering Research Council of Canada and the New Brunswick Innovation Foundation.

NOMENCLATURE

C_p	heat capacity, $J/kg.K$
D_{eff}	effective diffusion coefficient, m^2/s
G_m	specific gravity of wood
h	enthalpy, J/kg
J_v	fluxes of moisture, $kg/m^2.s$
J_e	fluxes of enthalpy, W/m^2
K	wood permeability, m^2
k_r	relative permeability
\dot{m}	moisture evaporation rate, $kg/m^2.s$
M	moisture content
M_{max}	moisture content with entire void structure filled by liquid.
p	pressure, Pa
Q	heat generation in wood, W/m^3
R	gas constant, $J / mol \cdot K$
T	wood temperature, K
u	velocity, m/s
ρ	density of liquid, kg/m^3
λ_{eff}	thermal conductivity, $W/m.K$
φ	void fraction in porous media

Superscripts

n	available values at last time step
$n+1$	the unknown at next time step

Subscripts

a	air; b bound water;
g	gas; l liquid;
s	solid; v vapor ;
T	transverse direction
L	longitudinal direction

REFERENCES

- Antti, A.L., 1992: Microwave drying of hardwood: Simultaneous measurements of pressure, temperature, and weight reduction. *Forest Prod. J.*, 42 (6): 49-54.
- Antti, A.L., 1995: Microwave drying of pine and spruce. *Holz als Roh- und Werkstoff*, 53: 333-338.
- Barnes, D.; Admiraal L.; Pike, R. L; Mathur, V. N. P., 1976: Continuous system for the drying of lumber with microwave energy. *Forest Prod. J.*, 26 (5):31-42.
- Blasi, C. D., 1998: Multi-phase moisture transfer in the high temperature drying of wood particles. *Chemical Engineering Science*, 53(2): 353-366.
- Gong, L.; Plumb, O.A., 1990: Non-homogeneous model for moisture transport in softwood during drying. *ASME, HTD*, 129: 139-148
- Jia, D., 2006: Numerical and experimental study of microwave drying of hardwood. M.Engg. Thesis, UNB.
- Koumoutsakos, A.; Avramidis, S.; Hatzikiriakos, S. G., 2001: Radio frequency vacuum drying of wood. I. Mathematical model. *Drying Technology*, 19(1): 65-84.
- Mardini, J.A.; Lavine, A.S.; Dhir, V.K, 1996: Heat and mass transfer wooden dowels during a simulated fire: An experimental and analytical study. *International Journal of Heat and Mass Transfer*, 39(13): 2641-2651.
- McAlister, W. R.; Resch, H., 1971: Drying 1-inch ponderosa pine lumber with a combination of microwave power and hot air. *Forest Products Journal*, 21(3): 26-34.
- Perre, P., 1996: The Numerical modeling of physical and mechanical phenomena involved in wood drying: An excellent tool for assisting with the study of new processes. 5th International IUFRO Wood Drying Conference Proceedings, 11-38.
- Perre, P.; Turner, I.W., 1999: The use of numerical simulation as a cognitive tool for studying the microwave drying of softwood in an over-sized waveguide. *Wood Sci. Technol.*, 33: 445-464.
- Siau, J. F. 1995: Wood: Influence of Moisture on Physical Properties. Virginia Tech.
- Spolek, G. A.; Plumb, O. A., 1981: Capillary pressure in softwoods. *Wood Science Technology*, 15(3): 189-199.
- Stanish, M.A.; Schajer, G.S.; Kayhan, F. A , 1986: Mathematical model of drying in hygroscopic porous media. *AIChE Journal*, 32(8): 1301-1311.
- Turner, I.W.; Ferguson, W.J., 1995: A study of the power density distribution generated during combined microwave and convective drying of softwood. *Drying Technology*, 13: 1411-1430.
- Whitaker, S., 1977: Simultaneous heat, mass and momentum transfer in porous media: A theory of drying. *Advances in Heat Transfer*, 13: 119-203.
- Zhao, H.; Turner, I.W., 2000: The use of a coupled computational model for studying the microwave heating of wood. *Applied Mathematical Modeling*, 24: 183-197.

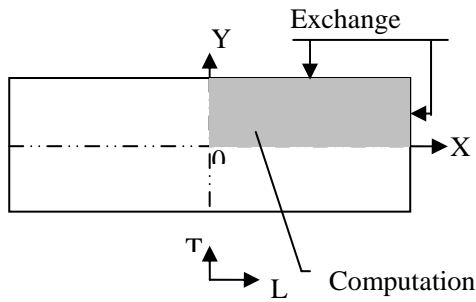


Fig.1 The 2-D model computation domain configuration

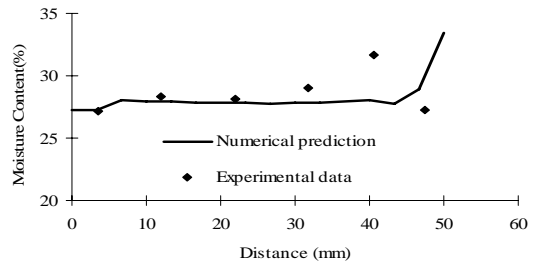


Fig. 5 Moisture distribution predicted in longitudinal direction @ average MC 28.7%, 250W

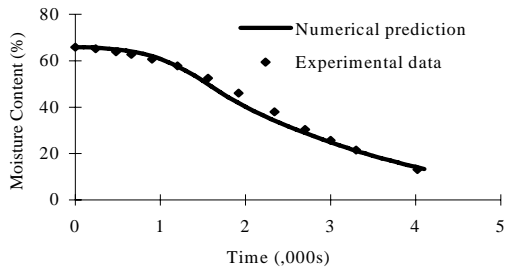


Fig. 2 Predicted drying curve at 250W.

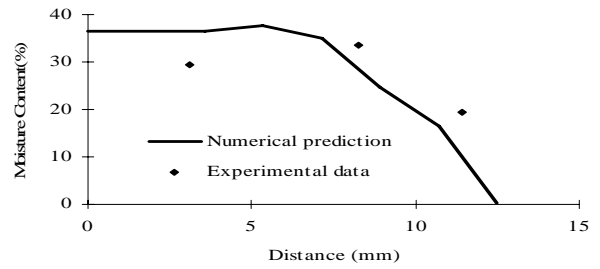


Fig. 6 Moisture distribution predicted in transverse direction @ average MC 28.0% , 250W

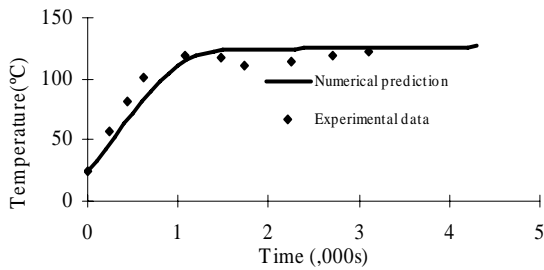


Fig. 3 Predicted temperature rise at 250W

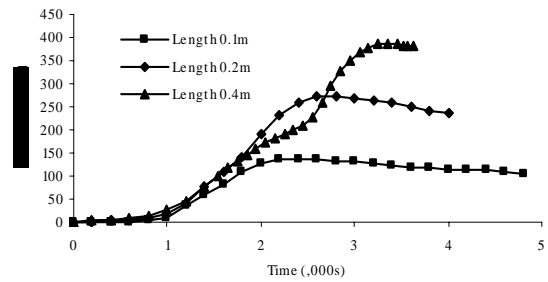


Fig. 7 Effect of specimen length on internal gaseous relative pressure

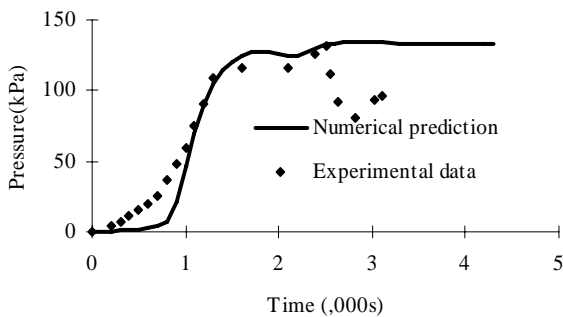


Fig. 4 Predicted internal gaseous relative pressure at 250W

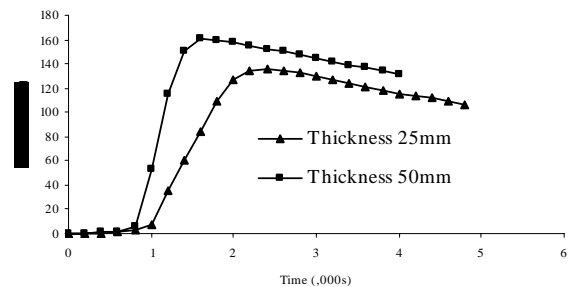


Fig. 8 Effect of specimen thickness on internal gaseous relative pressure